J Mater Sci (2011) 46:1767–1779
DOI 10.1007/s10853-010-4998-y

Multi-length scale modeling and analysis of microstructure evolution and mechanical properties in polyurea

Mica Grujicic · B. Pandurangan · A. E. King ·
J. Runt · J. Tarter · G. Dillon

Received: 8 July 2010 / Accepted: 8 October 2010 / Published online: 21 October 2010

Abstract A number of experimental investigations reported in the open literature have indicated that polyurea possesses a very complex nanometer-scale material microstructure consisting of hydrogen-bonded discrete hard (high glass-transition temperature, T_g) domains and a soft (low T_g) matrix and that the mechanical properties of this type of elastomer are highly dependent on the details of this microstructure. To help elucidate the internal processes/mechanisms associated with the microstructure evolution and to improve the understanding of microstructure/properties in this material, a multi-length scale approach is developed and utilized in the present work. This approach combines well-established and validated atomic, meso, and continuum length-scale techniques and spans around six orders of magnitude of length (from nanometers to millimeters). While within the atomic-scale approach, the material is modeled as a collection of constituent atom-size particles, within the meso-scale approach this atomistic description of the material is replaced with a collection of coarser particles/beads which account for the collective degrees of freedom of the constituent atoms. One of the main efforts in the present work was the derivation of accurate input parameters for meso-scale simulations from the associated atomic-scale material model and results. The meso-scale analysis provided critical information regarding the material microstructure and its evolution (from an initially fully blended homogeneous state). To obtain quantitative relationships between material microstructure and its mechanical properties, the computed meso-scale material microstructures are combined with a finite element approach. The predictions of the present multi-scale computational approach are found to be in good overall agreement with their experimental counterparts.

Introduction

Polyurea falls into a class of microphase-segregated and thermoplastically cross-linked elastomeric co-polymers (the terms “microphase-segregated” and “thermoplastically cross-linked” will be defined later) that are formed by the rapid chemical reaction between isocyanates (organic chemicals containing isocyanate –N=C=O groups) and amines (organic chemicals containing amine $–NH_2$ groups). A schematic of the polyurea co-polymerization reaction is shown in Fig. 1 in which symbol R is used to represent an aromatic functional group (e.g., diphenyl methane) while R′ is used to denote an aromatic/aliphatic long chain functional group (e.g., polytetramethylene-oxide-di-phenyl). Since the co-polymerization/gel reaction times are typically less than a minute, polyurea synthesis can be achieved under a wide range of temperatures and humidity without significantly affecting material microstructure and properties.

An examination of Fig. 1 reveals that the co-polymerization reaction creates urea linkages which are polar, i.e., contain centers/poles of negative and positive charge. Also seen in Fig. 1 is that urea linkages together with the R

M. Grujicic (✉) · B. Pandurangan · A. E. King
Department of Mechanical Engineering, Clemson University,
241 Engineering Innovation Building, Clemson, SC 29634-0921, USA
e-mail: mica.grujicic@ces.clemson.edu

J. Runt
Department of Material Science and Engineering, Pennsylvania State University, University Park, PA 16082, USA

J. Tarter · G. Dillon
Applied Research Laboratories, Pennsylvania State University, University Park, PA 16082, USA

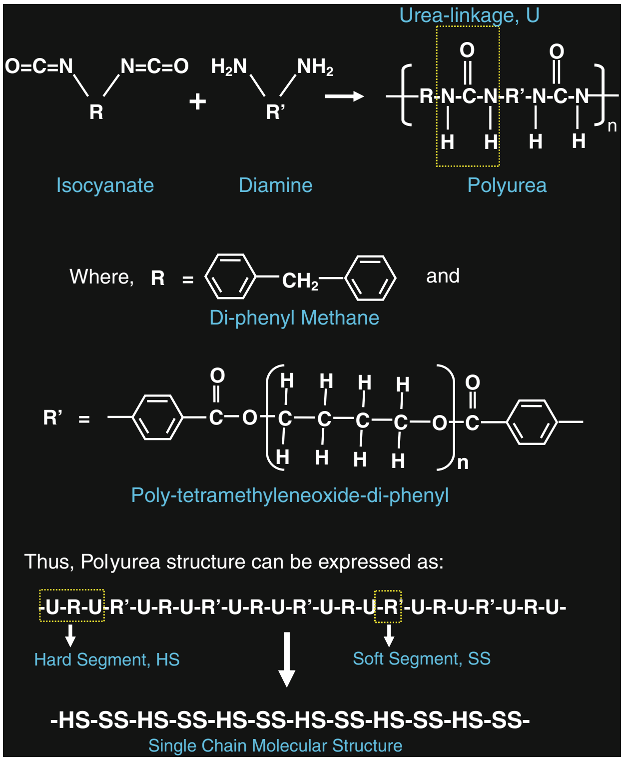

Fig. 1 Co-polymerization reaction resulting in the formation of segmented polyurea. To simplify the schematic of the molecular structure, symbols *HS* (hard segment) and *SS* (soft segment) are used

functional groups form the so-called “hard segments” (denoted as HS) within individual polyurea chains. Within the same chains, R′ functional groups form the so-called “soft segments” (denoted as SS). As a result of strong hydrogen bonding between urea linkages of the neighboring chains (or the neighboring portions of the same chain), hard segments are typically micro-phase segregated into the so-called “hard domains”. An example of the formation of hard domains within polyurea is shown schematically in Fig. 2. As shown in this figure, non-phase-segregated hard segments and soft segments form a soft (i.e., low glass transition temperature, T_g) matrix. Since hydrogen bonding provides inter-chain joining, polyureas are often referred to as being thermoplastically cross-linked (in contrast to more commonly covalently cross-linked) polymers. Consequently, polyureas are described as segmented (segment-containing) and thermoplastically cross-linked (hydrogen bonding provides chain cross-linking) elastomers. The hard domains typically possess a high glass transition temperature (T_g) and can crystallize under suitable thermo-mechanical processing conditions [1]. Also, it should be noted that these domains act not only as thermoplastic cross-links but also as rigid reinforcements within the continuous low T_g, compliant, and soft matrix.

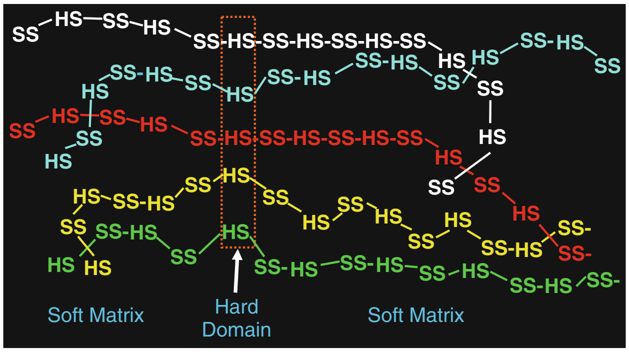

Fig. 2 Schematic representation of the formation of hard domains and the soft matrix within polyurea

Due to their highly complex internal microstructure described above, polyureas display a very broad range of mechanical responses under static and dynamic loading conditions. The main features of these responses can be defined as: (a) a high-level of stress versus strain constitutive non-linearity; (b) extreme strain-rate (and temperature) sensitivity; and (c) a high degree of pressure dependence. These types of mechanical responses have favored the use of polyurea as an abrasion/corrosion protection and blast/ballistic-impact mitigation material. For instance, polyureas are frequently used as:

(a) Tough, abrasion-resistant, corrosion-resistant, durable, and impact-resistant (epoxy/rubber replacement) spray-on coatings/liners in various construction/structural applications such as tunnels, bridges, roofs, parking decks, storage tanks, freight ships, truck beds, etc.;
(b) External and internal wall-sidings and foundation coatings for buildings aimed at minimizing the degree of structure fragmentation and, in turn, minimizing the extent of the associated collateral damage in the case of a bomb blast; and
(c) Gun-fire/ballistic resistant and explosion/blast mitigating coatings/liners or inter-layers in blast-resistant sandwich panels for military vehicles and structures.

The applications mentioned above capitalize on the exceptional ability of polyureas to harden under applied loading and to alter/disperse shock waves and absorb the kinetic energy associated with these waves/ballistic projectiles (under dynamic loading conditions) [2, 3]. While it is generally accepted that the high abrasion resistance and the superior blast/ballistic-impact mitigation performance of polyureas is the result of their intrinsic microstructure [4], details regarding the relationships between the material microstructure and the associated molecular-level processes and the macroscopic mechanical response of the polyurea are not presently well understood.

In order to help gain insight into the molecular-level microstructure and processes and their effect on the macroscopic mechanical response of polyurea, a multi-length/time scale procedure is introduced and employed in the present work. To help understand the proposed multi-length/time scale procedure, a flow chart is depicted in Fig. 3. It is seen that the procedure employs atomic-level methods, meso-scale level calculations and continuum-level finite element analysis. While ab initio quantum mechanics methods have the advantage that they can, in principle, be used for any element in the periodic table without specific parameterization, they have a serious short-coming since they can be employed only for systems containing no more than a few hundred atoms/particles. As will be shown below, while ab initio quantum mechanics calculations are not directly used in the present work, some of the computational ab initio quantum mechanics results are used in the parameterization of the material model at the atomic length/time scale.

Fully atomistic computational methods, like the ones used in the present work, in which each atom is uniquely identified, rely on the application of molecular mechanics, dynamics, and Monte Carlo algorithms to quantify the response of polymeric materials. While most material properties can be inferred from the application of these methods, determination of the properties that are fundamentally electronic (e.g., polarizability, dielectric constant, rates of chemical reactions, etc.) typically entails the use of either ab initio quantum mechanics or meso-scale computational methods. The accuracy of properties predicted by the atomic-level computational methods is greatly dependent on accuracy and fidelity of the employed force field (the mathematical expression used to create the potential function of the interacting particles). In the present work, the so-called "COMPASS" (Condensed-phase Optimized Molecular Potentials for Atomistic Simulation Studies) force field is used [5, 6]. This highly accurate force field is of an ab initio type since most of its parameters were determined by matching the predictions made by the ab initio quantum mechanics calculations to the condensed-matter experimental data. In passing, it should be recognized that the COMPASS force field is a prime example of how the highly accurate results obtained on one length/time scale (quantum mechanic/electronic, in the present case) and the experimental data can be combined to parameterize material models used at coarser length/time scale (the atomistic length/time scale, in the present case).

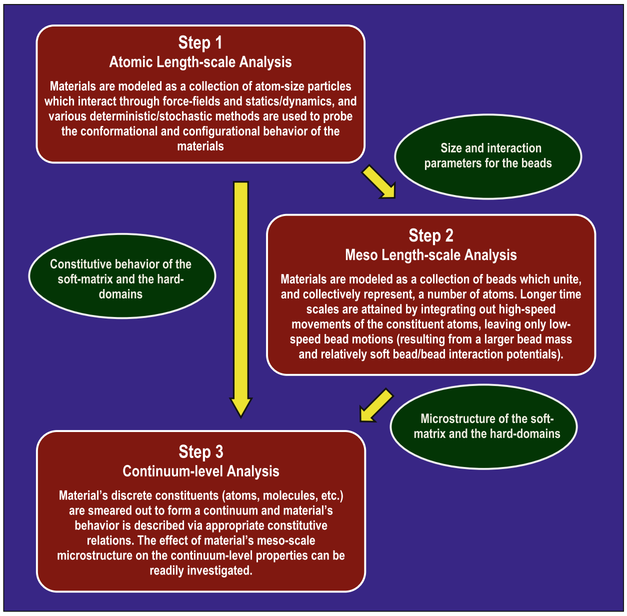

Materials are modeled as a collection of atom-size particles which interact through force-fields and statics/dynamics, and various deterministic/stochastic methods are used to probe the conformational and configurational behavior of the materials

Materials are modeled as a collection of beads which unite, and collectively represent, a number of atoms. Longer time scales are attained by integrating out high-speed movements of the constituent atoms, leaving only low-speed bead motions (resulting from a larger bead mass and relatively soft bead/bead interaction potentials).

Material's discrete constituents (atoms, molecules, etc.) are smeared out to form a continuum and material's behavior is described via appropriate constitutive relations. The effect of material's meso-scale microstructure on the continuum-level properties can be readily investigated.

Fig. 3 A flow chart of the multi-length/time scale computational procedure proposed in the present work

Within the fully atomistic methods described above, materials response/properties are derived under the conditions of constant material density, chemical composition, and structure. Hence these methods are inherently suitable only for pure (one component) or well mixed (multi-component) systems. When the system is multi-componental, with limited component solubilities and the chain topologies are highly complex, exotic phases are often formed. Since these so-called "mesophases" comprise a large number of items, their formation and properties cannot be efficiently modeled using fully atomistic computational methods. Instead, the so-called "coarse-grained" meso-scale computational methods become more suited in these types of calculations. In these methods, longer length scales are achieved by uniting many atoms into a single entity called "bead" (each bead represents the collective degrees of freedom of the constituent atoms) while longer time scales are obtained by integrating out the high speed movements of the constituent particles/atoms. This leaves only the soft bead/bead interactions and low speed movements of the beads. Hence, these methods are suitable for studying more sluggish micron-scale phase separation phenomena such as the formation of hard domains and the soft matrix in polyurea. It is critical to note that in order for the meso-scale methods to yield reliable predictions, the bead/bead interaction potentials must capture, in a meaningful way, the underlying interactions of the constituent atoms. Consequently, full atomic-scale computational methods are used to parameterize the meso-scale bead/bead interaction potentials. This is another example of how the highly accurate results obtained on one length/time scale (the atomistic length/time scale, in the present case) and the experimental data can be combined to parameterize material models used at coarser length/time scale (meso length/time scale, in the present case).

The main outcome of meso-scale computational analysis is the prediction of the phase morphologies with characteristic dimensions of the order of microns. While these morphologies are of great interest, meso-scale computational methods offer relatively little in terms of the prediction of the associated physical and mechanical properties of the material. To obtain these properties, one can combine meso-scale predicted phase-morphology results with a continuum-level finite element computational analysis. In this way, one can obtain a direct link between the atomic and meso length/time scale material microstructure and the macro-scale material properties.

The organization of the paper is as follows: a brief overview of the unit cell geometry and microstructure, the computational method and the associated problem statement for the atomic-scale, meso-scale and continuum-scale analyses are presented in "Atomic-scale calculations", "Meso-scale calculations", and "Continuum-scale calculations" sections, respectively. The main results obtained in the present work are presented and discussed in "Results and discussion" section, while the key conclusions resulted from the present study are summarized in "Summary and conclusions" section.

Computational procedure

Atomic-scale calculations

Formulation of an atomic-scale simulation problem requires, at a minimum, specification of the following three aspects: (a) an atomic-scale computational model consisting of atoms, ions, functional groups, and/or molecules; (b) a set of interaction potentials (commonly referred to as force fields) which describe accurately various bonding and non-bonding interaction forces between the constituents of the atomic-scale model; and (c) a computational method(s) to be used in the simulation. More details of these three aspects of the atomic-scale modeling and simulations of polyurea are provided below.

Computational model

The first step in the atomic-scale computational analysis was the construction of a single polyurea molecule. This was carried out using the Visualizer [7] program from Accelrys. A close-up view of a typical polyurea molecule obtained is shown in Fig. 4a. For clarity, different atomic

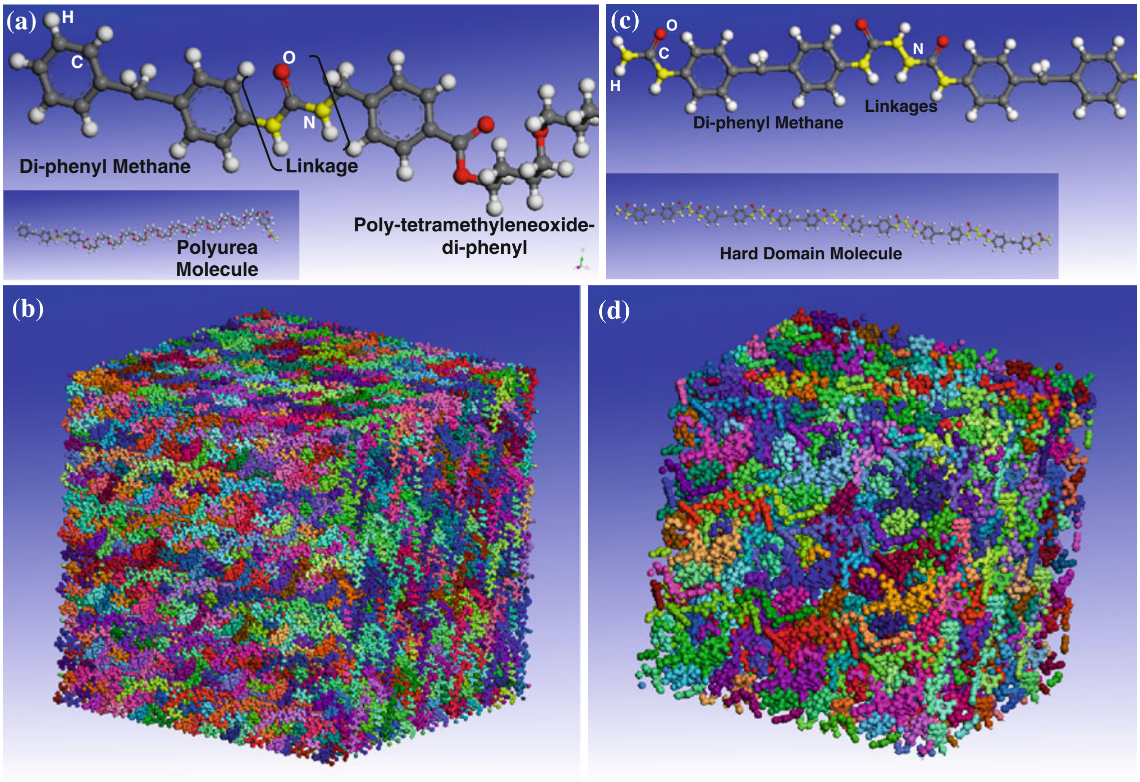

Fig. 4 **a** A segment of a single polyurea molecule with the *inset* showing a zoomed-out view of the same molecule; and **b** the atomic-scale computational unit cell in which, for clarity, each molecule is assigned a unique color

species and functional groups are labeled in this figure. Also, a zoomed-out view of a single polyurea molecule is shown as an inset in Fig. 4a. It should be noted that the polyurea molecule analyzed in the present work is based on an isocyanate consisting of diphenyl methane (R) functional group and a diamine consisting of polytetramethyleneoxide-di-phenyl (R') functional group (consisting of 14 C_2H_8O units), to comply with the type of polyurea being investigated experimentally in our ongoing work.

In order to model the behavior of bulk polyurea (i.e., in the absence of any free-surface effects) at the atomic length scale, a rectangular box-shaped computational unit cell is constructed and the periodic boundary conditions are applied across the faces of the cell. The three edges (a, b, and c) of the cell are aligned, respectively, with the three coordinate axes (x, y, and z). The atomic configuration within the cell containing polyurea chains whose construction was described in the previous section is generated using the following procedure:

(a) The molecular chain constructed above is first grown by a copy-and-attach process to increase its length/molecular weight;

(b) The single polyurea chain constructed in (a) is next used within the Amorphous Cell program from Accelrys [8] to fill the rectangular box-shaped computational cell of a preselected size (6.7 nm × 6.7 nm × 6.7 nm) while attaining the target density (1300 kg/m^3) of polyurea; and

(c) The atomic configuration obtained in (b) is optimized by minimizing its potential energy with respect to the positions of the constituent atoms.

An example of the atomic-scale computational cell used in the present work is displayed in Fig. 4b. This cell contains 11,745 atoms of carbon, 18,900 atoms of hydrogen, 540 atoms of nitrogen, and 2,565 atoms of oxygen.

As discussed earlier, as-synthesized polyurea is typically micro-phase segregated and consists of hard domains and a soft matrix. In contrast, the atomic-scale polyurea model as depicted in Fig. 4b represents a completely mixed state of this material. As will be discussed later in detail, within the atomic-scale computational methods used, micro-phase separation processes cannot be generally investigated. Hence, atomic-scale calculations based on the unit cell displayed in Fig. 4b can only provide information about the fully mixed material state/properties, i.e., information about the material which resembles the soft-matrix phase of polyurea. It should be recalled that, within the soft-matrix, hard and soft segments are well mixed and, hence, the atomic-scale material model depicted in Fig. 4b is a realistic representation of this phase of the polyurea. To obtain atomic-scale level information about the material state/properties within the hard domains of polyurea, a new molecule-type consisting of only hard segments and the corresponding unit cell are used, Fig. 4c, d, respectively.

Force fields

While accurate simulations of a system of interacting particles/atoms generally entail the application of quantum mechanical techniques, such techniques are computationally quite expensive and are usually feasible only in systems containing up to a few hundreds of interacting particles/atoms. In addition, the main goal of simulations of systems containing a large number of particles/atoms is generally to obtain the materials' bulk properties which are primarily controlled by the location of atomic nuclei. Hence, the knowledge of the electronic structure, which is the main outcome of the quantum mechanics computations, is not critical. Under these circumstances, a good insight into the behavior of a material system can be obtained if a reasonable, physically based approximation of the potential (force field) in which atomic nuclei move is available. Such a force field can be used to generate a set of material system configurations which are statistically consistent with a fully quantum mechanical description of the same system.

In the present molecular-level analysis of polyurea, COMPASS [5, 6] functional forms and parameterizations were used for various bond and non-bond interaction energies appearing in Eqs. 1–4. COMPASS is a set of force field potentials which were derived through the use of ab initio quantum mechanical calculations and has proven to be highly accurate and reliable in starting various organic/inorganic condensed matter problems. A schematic explanation of the first four types of valence atomic interactions included in the COMPASS force field is given in Fig. 5. A summary of the COMPASS force field functions can be found in our previous work [9].

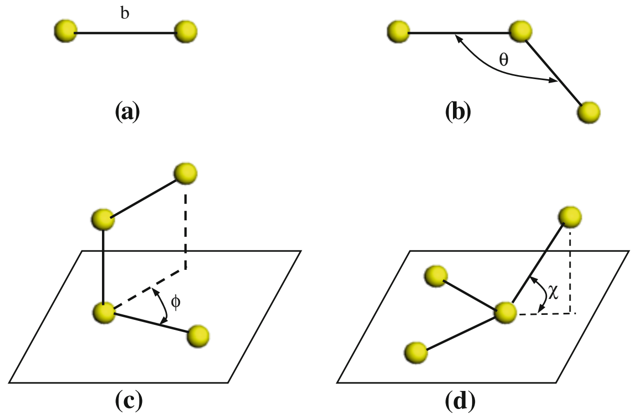

Fig. 5 A schematic of the: **a** stretch, **b** angle, **c** torsion, and **d** inversion valence atomic interactions

Computational method

Both molecular statics and molecular dynamics simulations were employed in the present work. Within the molecular statics approach, the unit cell potential energy (as defined by Eqs. 1–4) is minimized with respect to the position of the constituent particles/atoms. The potential energy minimization within Discover [10] (the atomic simulation program from Accelrys used in the present work) is carried out by combining the Steepest Descent, Conjugate Gradient, and the Newton's minimization algorithms. These algorithms are automatically inactivated/activated as the atomic configuration is approaching its energy minimum (i.e., the Steepest Descent method is activated at the beginning of the energy minimization while the Newton's method is utilized in the final stages of the energy minimization procedure).

Within the molecular dynamics approach, gradient of the potential energy with respect to the particle positions is first used to generate forces acting on the particles and, then, the associated Newton's equations of motion (for all particles) are integrated numerically to track the temporal evolution of the particle positions. More details regarding the use of Discover to carry out molecular statics and molecular dynamics analyses can be found in our prior work [9].

Determination of the room-temperature atomic-level mechanical properties of the two phases (soft matrix and hard domains) within polyurea is accomplished by carrying out the appropriate deformation of the computational cell followed by combined application of molecular statics and molecular dynamics analyses. These simulations yielded a functional relationship between the internal energy and the deformation state of the unit cell. As will be discussed in detail in "Results and discussion" section, the mechanical response of the two polyurea phases is obtained by appropriate differentiation of this function. It should be noted that while this procedure accounts for the contribution of deformation to both the (bonding and non-bonding) potential and vibrational energy components, changes in the (configurational) entropy are not accounted for. To assess the consequence of this simplification, the approach described in Ref. [11] was considered. This approach defines a dimensionless parameter and states that when this parameter is significantly smaller than unity, entropy effects can be neglected. Unfortunately, detailed temperature and pressure dependencies of the material mechanical response of polyurea needed to evaluate this parameter were not available. Hence, the approach could not be implemented.

The aforementioned deformations of the atomic-scale computational cell are carried out through the use of a Discover input file [10] which is written in a Basic Tool Command Language (BTCL) language. This enabled the use of a scripting engine that provides very precise control of simulation jobs, e.g., a cell deformation to be carried out in small steps each followed by a combined energy-minimization/molecular-dynamics simulation run. The energy minimization procedure allows the system to reach the condition of a minimum potential energy while the subsequent molecular dynamics simulation enables the calculation of the average potential and vibrational energies. Typically, conventional *NVT* ($N = 33{,}750$, the number of particles; $V = 6.7^3$ nm^3, computational cell volume; and $T = 298$ K, temperature; all kept constant) molecular dynamics method was employed with 10,000 1.0 fs time steps.

Problem formulation

As discussed earlier, atomic-scale computational methods used here are not suitable for the investigation of microphase separation processes. The main reasons for this are as follows:

(a) Within the molecular statics, local minimization algorithms are employed which are capable of only finding a minimum energy configuration of the given (fully mixed or hard-domain) state of the material; and
(b) Molecular dynamics is dominated by high frequency atomic vibrations and unrealizable computational times are needed to simulate phase separation using this approach.

Taking the above into consideration, atomic-scale calculations are employed in the present work for two main purposes: (a) to generate the necessary parameters for use in the meso-scale computational analysis; and (b) to determine local mechanical properties of the soft matrix and the hard domains within polyurea.

Meso-scale calculations

Within the meso-scale computational approach, the atomic-scale description of the molecules is coarse-grained to form the so-called "beads" which represent the collective degrees of freedom of all the constituent atoms. These beads interact through pair-potentials which, in order to obtain meaningful results, must capture the underlying interactions between the constituent atoms. The procedures, used to construct the appropriate meso-scale computational unit cell and to derive bead–bead interaction potentials from the corresponding atomic-scale models and results, are discussed in this section.

All the meso-scale calculations carried out in the present work employed the so-called Mesodyn computational method [12, 13]. At the meso-scale, the material system is defined by prescribing bead properties (e.g., size/mass), architecture of the polymer chains (e.g., chain length, branching, etc.), and various bead mobility and interaction parameters (e.g., bead self-diffusion coefficients and the inter-chain Flory–Huggins non-ideal interaction parameters). The temporal evolution of the system is governed by a set of the so-called "functional Langevin equations" (one for each bead-type) which are numerically solved. More details regarding the Mesodyn computational method are provided later in this section.

Computational cell

In order to model the behavior of a bulk material system, an analogous approach was taken as in the case of atomic-scale calculations. That is, a rectangular box-shaped computational cell (with an edge length which is approximately an order of magnitude larger than its atomic-scale counterpart) was constructed and the periodic boundary conditions applied to all of its faces. An example of the conversion of the atomic-scale material model into the corresponding meso-scale material model is displayed in Fig. 6a, b. In Fig. 6a, a segment of the meso-scale molecular chain consisting of two bead types: A (red) and B (blue), is displayed. The nature of the two beads will be discussed later. In Fig. 6b, an example is provided of the corresponding meso-scale unit cell used in the microstructure-evolution analysis of bulk polyurea.

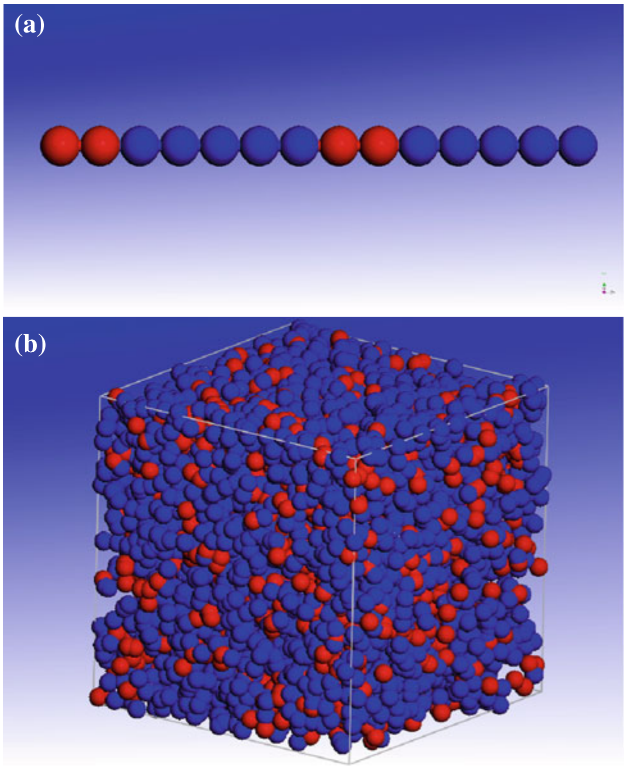

Fig. 6 **a** A segment of the meso-scale model for a single Gaussian-chain of polyurea consisting of two types of beads A (*red/light*) and B (*blue/dark*); and **b** the meso-scale computational unit cell used to model bulk polyurea (Color figure online)

The mesodyn computational method

As mentioned earlier, all the meso-scale calculations carried out in the present work employed the so-called Mesodyn computational method [12, 13]. Within this method, polymer molecules are defined as "Gaussian chains of beads". A Gaussian chain consists of orientationally uncorrelated (freely jointed) links with the link lengths (adjacent bead separation distances) following a particular Gaussian-related statistic. From the knowledge of the expectation value for the link lengths, a distribution of the end-to-end chain lengths can be readily derived for the Gaussian chains (using a random-walk method). This, in turn, leads to the determination of the corresponding configurational entropy and for a given intra-chain Hamiltonian (an energy function which depends on the distance of adjacent beads within the same chain) the corresponding free energy.

Within the Mesodyn method, the temporal evolution of the system is described by a set of so-called "functional Langevin equations". Essentially, these equations represent bead number density diffusion equations for different components (bead types) in the material. However, in contrast to the common diffusion equations, these equations each contain a random noise term (which enables the system to escape a local free-energy minimum associated with a metastable state of the system). Within the Mesodyn method, the driving force for bead number density evolution is the existence of a non-zero gradient of the corresponding intrinsic chemical potential. The later is obtained by differentiating the free energy functional with respect to the corresponding bead number density field. Temporal evolution of the component's density (from the initially homogeneous mixture), is computed by numerically inverting the Langevin equations.

The Mesodyn computational method is based on a dynamic variant of mean-field density functional theory which postulates that the free energy, F, of a heterogeneous material system is a functional of the local bead number density field, ρ and that there is a one-to-one correspondence between the bead spatial-distribution function in the system, the material density field and an externally applied potential field (a field-type lagrangian-multiplier function). Since the free energy is a thermodynamic potential, all other thermodynamic quantities can be derived from it through proper differentiation and the associated thermodynamic processes analyzed. For example, phase separation can be detected by monitoring spatial distribution of the bead number density within the system.

All the meso-scale computational analysis carried out in the present work were done using Mesodyn computer program from Accelrys [13].

Derivation of the meso-scale material model parameters

In this section, details regarding the derivation of the two key meso-scale material-model parameters (i.e., bead's size/length along the chain and the Flory–Huggins interaction parameter between beads) are presented.

Bead-size/length determination Before the bead lengths could be determined, one must select the atomic make-up of the beads and the number of bead types. As mentioned earlier, in order to keep the meso-scale material model relatively simple, the system is assumed to consist of two bead types (A and B). Based on the polyurea chain molecular-level structure (e.g., Fig. 1), it was decided to define two A beads as an assembly of one R functional group surrounded by two urea linkages and then by two phenyl groups (it should be noted that the latter are components of the R′ functional group, Fig. 1). Before the molecular-level structure of the bead B can be determined, it had to be recognized, as will be shown below, that the volumes of beads A and B have to be comparable. In order to determine the volume of the bead A, a series of molecular dynamics calculations were carried out using polyurea chains with the number of repeat C_4H_8O units within the R′ functional group increasing between 14 and 30. Volumes of the bead A and the C_4H_8O repeat units are then calculated from the resulting material specific volume change under the assumption that this specific volume is a linear combination of the (constant) specific volumes of these two species. Using this procedure, it was determined that the volume of three C_4H_8O repeat units ($3 \times 71.23 = 213.69$ cm^3/mol) is approximately equal to the volume of one A bead (1×209.8 cm^3/mol). Based on this finding, meso-scale Gaussian chains were assigned the following structure: A–A–B–B–B–B–B–A–A–B–B–B–B–B…. The same procedure identified an average bead length along the chain of 1.6 nm.

Determination of bead–bead interaction parameters Bead/bead Flory–Huggins interaction parameters are determined in the present work using the so-called Hildebrand's formula [14]. Within this formula, the Flory–Huggins interaction parameter χ_{AB} is given by:

$$\chi_{AB} = \frac{(\delta_A - \delta_B)^2}{RT} V_{ref} \tag{1}$$

where V_{ref} is the reference (i.e., the mean) volume of interacting beads and δ_I (I = A, B) is the bead solubility parameter. The latter is equal to the square root of the corresponding bead volumetric cohesive-energy density, where the bead cohesive energy density is a measure of the potential energy decrease, per unit volume, in a polymeric material system due to non-bond inter-chain interactions.

To determine the cohesive energy densities for the two beads, a series of molecular dynamics calculations are carried out, one based on 20 A-bead long molecular chains and the other based on 50 B-bead long molecular chains. The respective cohesive energy densities are obtained by averaging the molecular dynamics-based values calculated over a time period of 1 ns. The resulting cohesive energy density values (260.05 and 71.73 J/cm^3) for beads A and B, respectively, were validated using Synthia computer program from Accelrys [15] which employs the so-called Quantitative Structure Activity and Property Relationships (QSAR/QSPR) semi-empirical method to calculate physicochemical properties of polymers using the information about their topology. The cohesive energy density results obtained using Synthia were 285.05 and 68.73 J/cm^3 for beads A and B, respectively. In all the subsequent calculations, cohesive energy densities were set equal to the values obtained by averaging the molecular dynamics-based and Synthia-based values. The procedure employed in this section yielded an average value of the A-bead/B-bead unit-less Flory–Huggins interaction parameter of 5.42. The corresponding mean-field energetic interaction between beads is then calculated by multiplying this value of the Flory–Huggins parameter with the product of the universal gas constant and absolute temperature and by dividing the result by V_{ref}.

Problem formulation

Since the primary output of meso-scale modeling is the prediction of nanometer-to-micron-scale phase separation phenomena, it is used in the present work to study the formation of hard domains (and the soft matrix) from the initially homogeneous state of polyurea. As mentioned earlier, physical and mechanical properties of polyurea are highly sensitive to the details of its microstructure while the microstructural details are also highly sensitive to the polyurea chemistry. Hence, the use of the meso-scale computational method offers an opportunity for elucidating relationships between the material chemistry and its microstructure (and, to a lesser extent, relationships between materials microstructure and its properties). An example of a typical phase-separated meso-scale microstructure obtained in the present work is displayed in Fig. 7a.

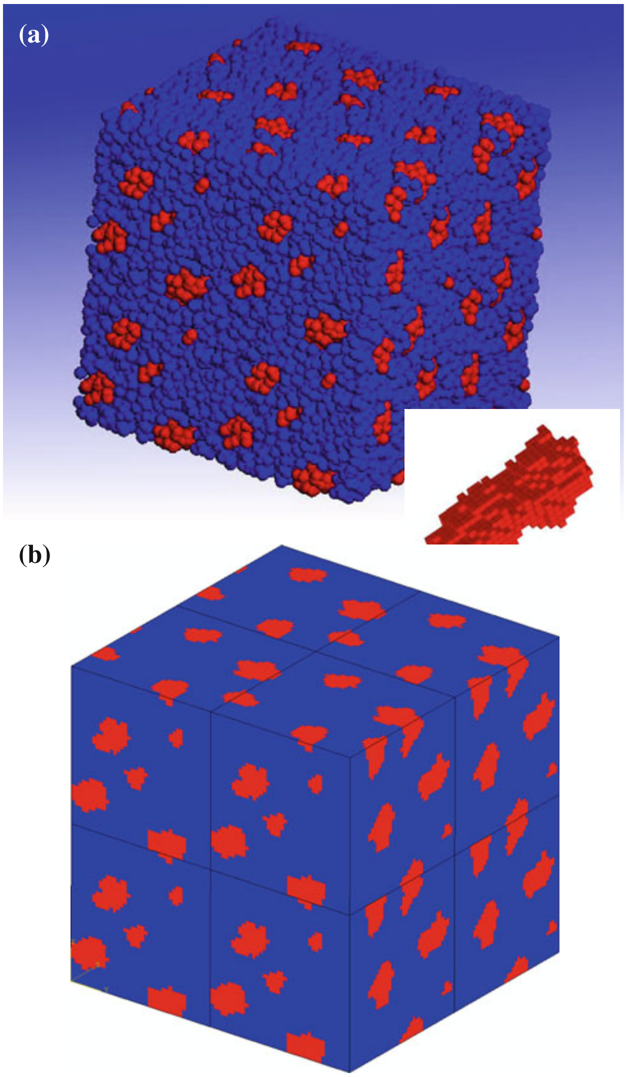

Fig. 7 **a** A nanometer-to-micron scale two-phase microstructure obtained using the meso-scale computational analysis; and **b** the corresponding finite element model

Continuum scale calculations

As mentioned above, the primary results of meso-scale analysis pertain to the prediction of the material nanometer-to-micron scale microstructure. To establish quantitative relations between such microstructure and the material (effective) properties, continuum-level approaches are used in conjunction with the material constitutive relations for the two constituent phases (as derived via the use of atomic-scale calculations). There are several well-established continuum-level methods for computation of the effective material properties (e.g., [16, 17]). In the present work, a modified version of the method described in Ref. [16] is utilized.

Computational cell

The first step in the present continuum-level computational procedure involves mapping of the meso-scale material microstructure onto a finite element mesh. The finite element mesh used in the present work consists of eight-node cubic elements (“voxels”). The edge length of the voxels is chosen to be a relatively small fraction of the bead length. During mapping of the discrete bead-based meso-scale microstructure into the corresponding continuum finite element model, each voxel is filled with material associated with a bead whose center-point is closest to the center-point of the voxel in question. To reduce stress concentrations associated with the step/terrace character of the hard-domain/soft-matrix interface, a procedure is devised to smooth-out these interfaces by controlled distortions of the voxels. An example of the typical phase-segregated continuum-level microstructure obtained in the present work is displayed in Fig. 7b. A close similarity between the meso-scale computational cell displayed in Fig. 7a and the corresponding finite-element computational cell shown in Fig. 7b is apparent.

The continuum-scale computational method

To determine the effective properties of the microphase-segregated polyurea, the computational cell displayed in Fig. 7b is subjected to a number of quasi-static deformation modes (while imposing periodic boundary conditions across the cell faces) and the corresponding stress versus strain curves are generated. More details regarding the deformation modes used will be presented in “Results and discussion” section, while additional details regarding the finite element method employed can be found in Ref. [16]. All calculations carried out in this portion of the work employed ABAQUS/Standard, a commercial (static) finite element package [18].

Continuum-level constitutive relations for the two constituent phases

As will be shown in “Continuum-level calculations” section, the material constitutive models for the soft matrix and the hard-domain materials were found to be available within the ABAQUS/Standard material library and, hence, the atomic-scale results only provide the needed parameterization of these models.

Problem formulation

As mentioned above, the main task at the continuum-level was to carry out finite-element analysis of few basic deformation modes to determine effective properties of polyurea associated with its microstructure obtained through the use of meso-scale computational analysis.

Results and discussion

Atomic-scale calculations

As mentioned earlier, the two main objectives of using atomic-scale calculations were: (a) determination of the meso-scale morphological and interaction parameters; and (b) determination and parameterization of the material models for the soft matrix and the hard domains, the two main phases in bulk polyurea. Utilization of the atomic-scale calculations in conjunction with the objective (a) was discussed in "Meso-scale calculations" section, while their use in objective (b) will be discussed here.

To determine the mechanical properties of the two phases, the atomic-scale computational cell was subjected to a variety of deformation modes (e.g., uniaxial-strain tension/compression, plane-strain tension/compression, simple shear, etc.) over a relatively large range of strains. An example of the typical results pertaining to the molecular-level microstructure, in the soft matrix and the hard domains after axial tension and simple shear are shown in Fig. 8a–d.

Soft-matrix material model

The soft matrix was found to be capable of undergoing large elastic strains and, hence, was treated as a hyperelastic material. Strains are deemed as being elastic if deformation of the computational cell followed by its full restoration to the initial state does not result in any changes of the atomic nearest neighbors. Following standard practice [19], the volumetric internal strain energy density (strain-energy density, in the following) of this phase is assumed to be a function of the invariants (I_1, I_2, I_3) of the left Cauchy deformation tensor, B (= FF^T) where F is the deformation gradient and superscript T denotes a transpose. The deformation gradient F simply maps the initial undeformed computational cell into the corresponding deformed computational cell. The three B invariants are defined as:

$$I_1 = \mathrm{tr}(B) \tag{2}$$

$$I_2 = \frac{1}{2}\left[I_1^2 - \mathrm{tr}(B^2)\right] \tag{3}$$

$$I_3 = \det(B) \tag{4}$$

where tr and det are used, respectively, to denote trace and determinant operators.

The computed internal-energy density, W, data are used to derive a $W(I_1,I_2)$ function while recognizing that in the

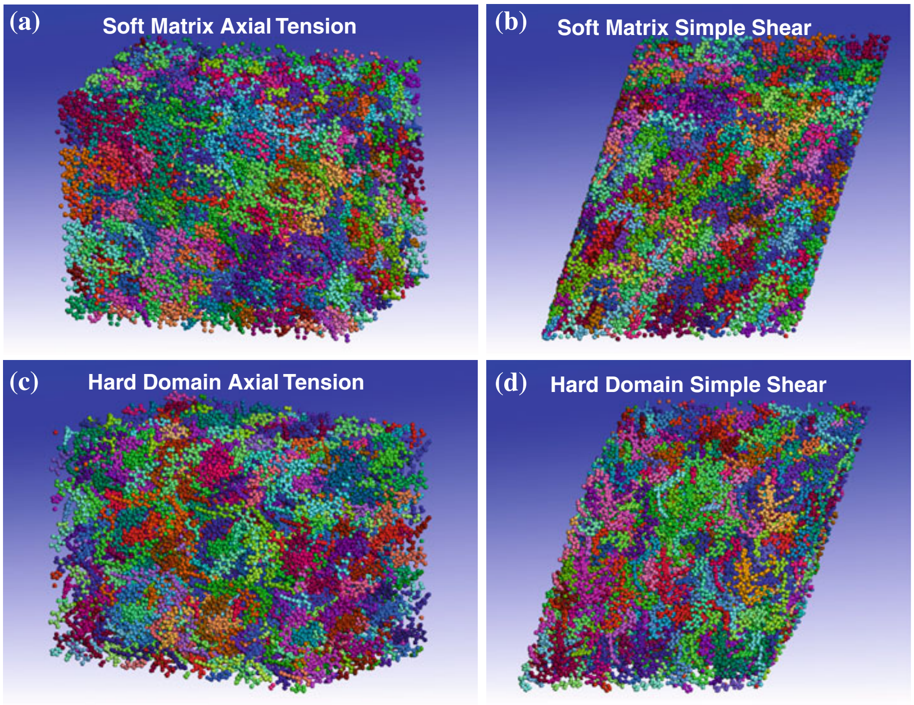

Fig. 8 Relaxed atomic configurations of the soft matrix (**a**, **b**) and the hard domains (**c**, **d**)within the computational cell after: **a**, **c** axial tension; and **b**, **d** simple shear

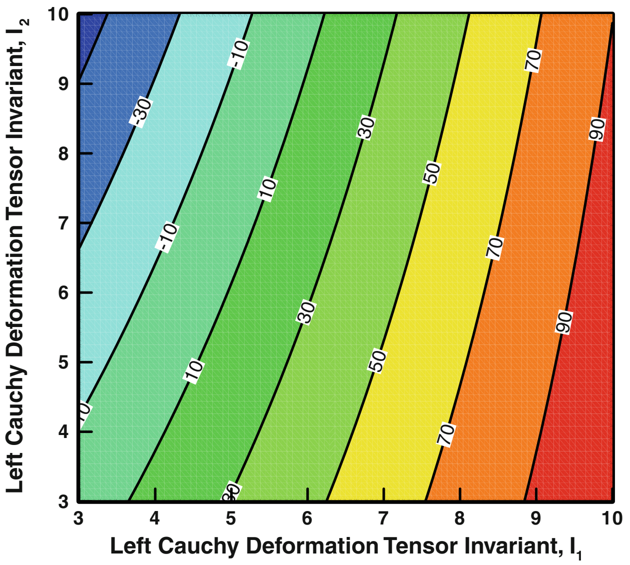

Fig. 9 A functional relationship between the strain energy density (MPa) and the first two invariants of the left Cauchy deformation tensor in the soft matrix of polyurea

nearly incompressible polyurea, $I_3 \sim 1.0$. The function was found to be consistent with the following truncated quadratic function of I_1 and I_2:

$$W(I_1, I_2) = c_1(I_1 - 3) + c_2(I_2 - 3) + c_3(I_1 - 3)(I_2 - 3) \tag{5}$$

with $c_1 = 15.4 \pm 1.1$ MPa, $c_2 = -8.44 \pm 0.7$ MPa, and $c_3 = 0.82 \pm 0.05$ MPa where the number following the ±symbol denotes one standard deviation of the quantity in question. A contour plot showing the obtained $W(I_1,I_2)$ relationship is displayed in Fig. 9. Once $W(I_1,I_2)$ function is defined, the corresponding Cauchy stress versus large-deformation (logarithmic) strain relation can be obtained by proper differentiation of Eq. 5 and through the use of chain rule [20].

Hard-domains material model

In the case of hard domains, it was found that, at relatively small strains, inelastic deformations begin to dominate the mechanical response of this material. Hence, this phase is modeled as an isotropic elastic–plastic material and the internal-energy density taken to be a quadratic function of the strain components (with zero constant and linear terms). For an isotropic linear elastic material, the quadratic coefficient (a fourth-order elastic-stiffness tensor) contains only two independent parameters (selected here as the Young's modulus, E and the Poisson's ratio, ν). These two parameters were obtained by subjecting the computational cell to a set of uniaxial stress deformations and by fitting the computed W value to the quadratic function mentioned above. This procedure yielded the following values: $E = 48 \pm 2.5$ MPa and $\nu = 0.38 \pm 0.03$. To validate these results, W values were also computed for the case of the computational cell subjected to simple shear. The resulting shear modulus, G, was found to be fully consistent with its expected value ($=E/2(1 + \nu)$).

As far as the flow-strength of hard-domains is concerned, no significant strain-hardening effects were observed and both uniaxial stress and simple shear deformation models yielded consistent yield strength values of 16.1 ± 2.3 MPa. It is generally believed that, at sufficiently large stresses/strains, real polyurea undergoes plastic deformation [20] and that this type of deformation is localized within hard domains. While, the hard domain yield strength is typically determined indirectly by fitting the experimental data for polyurea, this quantity is determined directly in the present work by carrying out atomic-scale computational mechanical tests on the hard-domain material.

Meso-scale calculations

As mentioned earlier, the main output of the meso-scale calculations is the nanometer-to micron scale material microstructure. Typical meso-scale computational results displayed in Fig. 7a reveal that the initially fully mixed homogeneous material has microphase-segregated into discrete "peanut-shaped" hard domains distributed within a continuous matrix. An example of the hard domain morphology is presented as an inset in Fig. 7. This morphology is fairly consistent with the one observed experimentally in our on-going research [21]. In addition, the characteristic size (5–20 nm in length, 3–5 nm lateral dimension) of the "peanut-shaped" hard domains observed in Fig. 7a is consistent with their experimental counterpart.

Continuum-level calculations

It is well established that the effective mechanical response of heterogeneous materials such as micro-phase segregated polyurea is dependent on the properties of the constituent materials and the material microstructure. In "Atomic-scale calculations" section, atomic-scale computational results were used to construct material models for the two bulk-polyurea constituents, i.e., the soft matrix and the hard domains. In "Meso-scale calculations" section, meso-scale computations were employed to generate micro-phase segregated microstructure of the polyurea. In this section, finite-element calculations are employed to determine the effective quasi-static mechanical properties of bulk polyurea and to compare the results with their experimental counterparts in order to provide a proof of concept. In these calculations, in accordance with the findings presented in

"Atomic-scale calculations" and "Meso-scale calculations" sections, the soft matrix is modeled as a polynomial-type hyperelastic material while the hard domains are treated as an isotropic linear-elastic/ideal-plastic material. Since these models are already available in ABAQUS/Standard, only their parameterization, as determined in "Atomic-scale calculations" and "Meso-scale calculations" sections had to be provided.

However, before this task can be accomplished, the procedure outlined in "Computational cell" section had to be employed to construct the appropriate two-phase finite element model. An example of the finite element model obtained using this procedure is displayed in Fig. 7b. By subjecting the computational cell displayed in this figure to a variety of deformation modes and by measuring its mechanical resistance to deformation (via the use of quasi-static finite-element analysis), one can gain a detailed insight into the (quasi-static) mechanical response of the microphase-segregated polyurea. In other words, the finite element analysis can be employed to carry out a variety of computational mechanical tests on the two-phase polyurea. To establish the validity of this approach, one must demonstrate that the results of these computational mechanical tests are consistent with their experimental counterparts. Such validation was carried out in the present work and its details are presented in the remainder of this section.

To validate the present computational mechanical-testing procedure, the (10^{-3} s^{-1} strain-rate) uniaxial compression loading/unloading tests carried out by Yi and Boyce [22] are simulated using the computational cell displayed in Fig. 7b and by performing the finite element computations. A comparison between the computational and the experimental results is shown in Fig. 10. It is seen that the computed loading/unloading stress–strain response displays similar behavior as that found experimentally by Yi and Boyce [22]. Specifically, in both the computed and the experimental results loading is initially associated with a stiff response of the material. At larger strains, both the computed and the experimental results show a gradual loss of stiffness due to interplay between the geometrical and material non-linear effects. A similar level of agreement is observed in the unloading behavior of polyurea. Namely, the rate of unloading is initially quite high and subsequently decreases as unloading proceeds. The quantitative agreement between the two sets of results, however, can be described as only fair. Overall, these findings are encouraging since no polyurea-based experimental data/parameters were used in the present computational approach.

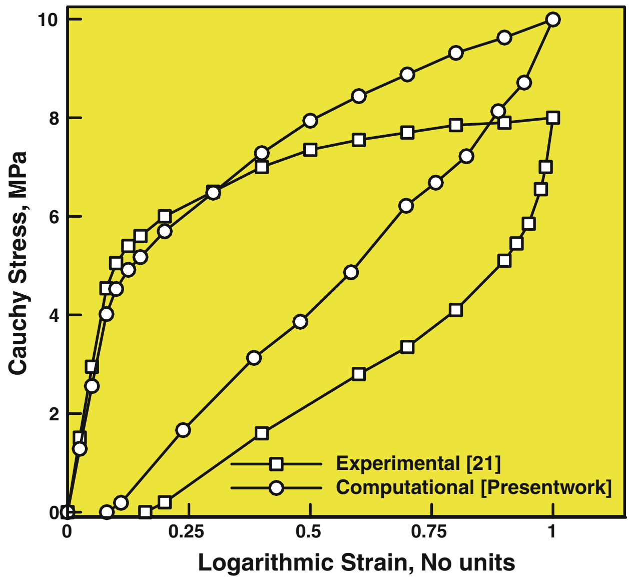

Fig. 10 A comparison between the quasi-static uniaxial compression stress versus strain results obtained experimentally in Ref. [22] and computationally in the present work

Future work

The procedure described above enables determination of the mechanical response of the two-phase polyurea unit cell subjected to any given state of deformation. Unfortunately, in most real-life computer aided engineering analyses such as interactions between an air-borne blast wave and a soldier's (helmet-protected or un-protected) head, impact of a projectile on to a polyurea-coated military vehicle body, etc., one cannot afford to use finely meshed unit cell-based finite-element models. Instead, a homogenized/smeared-out response of the two-phase polyurea is needed so that the number of elements in the finite-element mesh is manageable. Derivation of such a homogenized-material constitutive model is beyond the scope of the present work. Nevertheless, it should be noted that the results obtained in the present work can be used in two ways during derivation of such models: (a) atomic-scale-derived mechanical properties of the two phases and the meso-scale-derived material microstructure could be used as inputs to either a self-consistent, e.g., [23] or a so-called "generalized method of cells" (e.g. [24]) homogenization procedure; and (b) continuum-level finite-element results can be treated as "experimental" results and used in a more conventional "curve-fitting" procedure. Both of these approaches are being currently investigated in our on-going research and the results of this work will be reported in a future communication.

Summary and conclusions

Based on the results obtained in the present work, the following summary remarks and main conclusions can be drawn:

1. A three-step computational procedure combining atomic-scale, meso-scale, and continuum-level analyses of the material mechanical response and microstructure evolution is introduced and used to determine effective material properties of the micro-phase segregated polyurea.
2. At the atomic-scale, computational material tests are carried out to determine the mechanical response of the two polyurea phases, a soft matrix and the hard domains.
3. At the meso-scale, the process (and the product) of decomposition of an initially fully mixed polyurea into its two-phase segregated microstructure is carried out.
4. At the continuum-level, quasi-static finite element analyses are employed to determine the effective mechanical properties of the two-phase polyurea. The use of these results in constructing a homogenized (smeared-out) continuum-level material model for micro-phase separated polyurea is also discussed.

Acknowledgements The material presented in this paper is based on work supported by the Office of Naval Research (ONR) research contract entitled “Elastomeric Polymer-By-Design to Protect the Warfighter Against Traumatic Brain Injury by Diverting the Blast Induced Shock Waves from the Head”, Contract Number 4036-CU-ONR-1125 as funded through the Pennsylvania State University, the Army Research Office (ARO) research contract entitled “Multi-length Scale Material Model Development for Armor-grade Composites”, Contract Number W911NF-09-1-0513, and the Army Research Laboratory (ARL) research contract entitled “Computational Analysis and Modeling of Various Phenomena Accompanying Detonation Explosives Shallow-Buried in Soil” Contract Number W911NF-06-2-0042. The authors are indebted to Drs. Roshdy Barsoum of ONR and Bruce LaMattina of ARO for their continuing support and interest in the present work. The authors also want to thank professors J. Runt, J. Tarter, G. Settles, G. Dillon, and M. Hargether for stimulating discussions and friendship.

References

1. Ryan AJ (1989) Polymer 31:707
2. Grujicic M, Bell WC, Pandurangan B, He T (2010) J Mater Des. doi:10.1016/j.matdes.2010.05.002
3. Grujicic M, Pandurangan B, He T, Cheeseman BA, Yen C-F, Randow CL (2010) Mater Sci Eng A 527:7741
4. Roland CM, Cassini R (2007) Polymer 48:5747
5. Sun H (1998) J Phys Chem B 102:7338
6. Sun H, Ren P, Fried JR (1998) Comput Theoret Polym Sci 8(1/2):229
7. Materials Studio (2009) Visualizer Manual. Accelrys Inc., Princeton, NJ
8. Materials Studio (2009) Amorphous cell theory manual. Accelrys Inc., Princeton, NJ
9. Grujicic M, Sun YP, Koudela KL (2007) Appl Surf Sci 253:3009
10. Materials Studio (2009) Discover theory manual. Accelrys Inc., Princeton, NJ
11. Theodorou DN, Suter UW (1986) Macromolecules 19:139
12. Malcolm GN, Rowlinson JS (1957) Trans Faraday Soc 53:921
13. Materials Studio (2009) Mesodyn theory manual. Accelrys Inc., Princeton, NJ
14. Hildebrand JH (1919) J Am Chem Soc 41:1067
15. Materials Studio (2009) Synthia manual. Accelrys Inc., Princeton, NJ
16. Grujicic M, Zhang Y (1998) Mater Sci Eng A 251:64
17. Grujicic M, Cao G, Fadel GM (2002) J Mater Des Appl 215:225
18. ABAQUS/Standard Version 6.8-1 (2008) User Documentation, Dassault Systems
19. Grujicic M, Bell WC, Pandurangan B, Glomski PS (2010) J Mater Eng. doi:10.1007/s11665-010-9724-z
20. Grujicic M, Pandurangan B, He T, Hunt J, Tarter J, Dillon G (2010) J Mat Des Appl (submitted)
21. Runt J (2010) Research in progress, Pennsylvania State University
22. Yi J, Boyce MC, Lee GF, Balizer E (2006) Polymer 47:319
23. Bensoussan A, Lions JL, Panicolaou G (1978) Asymptotic analysis for periodic structures. North Holland, Amsterdam
24. Wilt TE, Arnold SM (1996) Micromechanics Analysis Code (MAC) User Guide: version 2.0., NASA TM-107290